15th IFK
Proc. of the 15th International Fluid Power Conference <Symposium/Conference>
<DOI>

Real-Time Fault Detection in Pneumatic Drive Applications Through Pattern Classification

Vladimir Boyko and Jürgen Weber

Chair of Fluid-Mechatronic Systems (Fluidtronics) – TUD Dresden University of Technology, Helmholtzstraße 7a, 01069 Dresden, Germany, vladimir.boyko@tu-dresden.de

Abstract.

Early fault detection in pneumatic systems is crucial for the prevention of unnoticed energy losses, high energy costs and system failures. According to various estimates, up to 40% of current compressed air consumption can be saved by locating and eliminating leaks. An increasing number of solutions for leakage detection have therefore been proposed in recent decades, which, however, are often cost-intensive, require the use of several additional sensors and cannot be transferred to other machines without extensive customization, leading to their low prevalence in industrial practice of cost-sensitive pneumatics.

This paper proposes a transferable fault detection method for pneumatic linear drives using only one pressure sensor per drive. By integrating neural networks and feature-based classification techniques, the method achieves up to 92.5% classification accuracy on the test dataset. For this purpose, extensive measurement data was generated for various systems and fault scenarios. Data features were extracted in the time and frequency domain using Python's “tsfresh” library and ranked using various feature selection methods such as recursive feature elimination or mutual information. Several classification methods, including Naive Bayes and k-nearest neighbors, were examined and compared with other classification methods such as neural network and cycle time-based fault detection. In this way, a real-time fault detection and localization method can be developed without interrupting machine operation to perform test cycles.

Keywords. Energy efficiency, compressed air systems, pneumatics, pneumatic actuators, fault detection, condition monitoring, energy loss, leakage, friction

1. INTRODUCTION

1.1. Current State

Compressed air is widely used as a practical and easily controllable energy source across many industrial applications. Pneumatic systems are regarded as cost-effective, durable, and environmentally sustainable automatization solutions capable of operating in demanding environments and relatively simple to install and maintain. However, one of the main drawbacks of pneumatic systems is their relatively high energy consumption. This has led to increased research efforts focused on improving their energy efficiency and developing reliable fault detection methods. Studies have shown that up to 40% of the energy used in pneumatics could be saved through more efficient system design and operation [1].

To realize this potential, several strategies are being pursued in science and industry. Primarily, these include demand-based sizing of components such as actuators, pipes, and compressors, as well as energy-saving circuits [2-7]. In parallel, there is growing attention on condition monitoring and fault detection systems. Recent studies [8,9] indicate that research on fault detection in pneumatic systems has grown considerably in recent years.

However, while many of the proposed approaches achieve reliable fault detection, they often require the integration of multiple additional sensors, making them economically impractical for pneumatic systems with numerous actuators [10]. Around 60% of the fault detection methods analyzed in [8,9] depend on the integration of multiple sensors to detect faults, e.g. several pressure and volume flow signals. Such solutions might provide more information and enable fault localization, but they are often not cost-effective for many companies, which limits their use in industry. Moreover, proposed monitoring concepts are often designed for a specific machine, requiring the methods and identified signal patterns to be extensively adjusted before being applied to a different system.

1.2. Commercially Available Fault Detection Solutions

In pneumatic drive systems, leakage and increased friction are the main sources of energy loss [11]. Detecting faults is challenging due to the robustness of pneumatic drives, which often remain functional even with severe issues like major leaks. Increased friction, caused by seal wear or uneven piston loads [12], is also hard to detect as it does not directly increase air consumption. At the same time, addressing leakages can save up to 40% of air consumption [1,13]. For this reason, numerous fault detection systems for pneumatic drives are available on the market; however, they still present several limitations.

Festo’s Motion Terminal (VTEM) offers a “Leakage diagnosis” application that performs a diagnostic test cycle to measure leakage volume flow based on cylinder volume, hose length, and pressure drop, halting operation during the test [14]. Similarly, the Festo MSE6-E2M device [15] and other systems such as [16] detect leaks by monitoring pressure drops in a blocked state or by using flow rate limits. However, such solutions lack fault localization without additional data such as valve actuation signals.

Ultrasonic leak detection allows testing without interfering with the system by using portable devices to sense air turbulences, but is less effective in large or hard-to-reach networks and cannot be used in operating systems due to exhaust noise [17-19]. Thermography is also conceivable, but requires expensive cameras and fails in complex machines where the pneumatic actuators are covered by other parts [20].

Friction from piston or guide wear is usually detected by monitoring pressure changes (which in general can also indicate leaks) or using special test rigs, which are not suitable for live systems [21]. High-frequency vibration analysis can identify increased friction during operation, but requires advanced equipment and protection [22,23].

Another monitoring concept that does not incur any additional costs, can be used during operation, and is therefore potentially suitable for industrial use is known as cycle time-based fault detection. The concept, first presented in [24] and expanded in [25,26], involves using proximity (reed) switches as soft sensors to detect deviations in the extension and retraction times of the pneumatic drive and to draw conclusions about possible fault sources. This allows faults within the pneumatic drive to be precisely localized. However, this approach is partially limited when monitoring highly dynamic drives with a pneumatic frequency ratio of $\Omega < 1.5$ according to [27].

1.3. Pressure-Based Fault Detection and Summary

The outlined state of the art indicates the demand for monitoring methods in pneumatic drive technology that can be applied across different systems and detect and localize faults during operation with minimum number of sensors. Such a low-cost and widely applicable approach based on cycle time was presented in [24,25], but it still has limitations in terms of distinguishability in some use cases. This paper therefore introduces another online method that uses the differential pressure signal (i.e., the difference between current and reference pressure) captured by a single sensor per drive and evaluated with various pattern classification techniques.

Pressure-based fault detection in pneumatic cylinders has been previously studied before (e.g., [23,28]), focusing mainly on analyzing pressure signals and a limited set of features such as min-max values or kurtosis. Moreover, the transferability of classifiers to different cylinder geometries or tasks as well as the influence of the sensor placement have rarely been examined. In the dissertation [11], the effects of three fault types (external/internal leakage and friction) on 32 algebraic features defined by the author, such as pressure difference and mean value, were analyzed using a pneumatic welding gun. This method requires prior training using a validated simulation model of the target system, which limits its direct transferability to other applications.

In his dissertation [10], Dierolf uses pressure, pressure difference, and flow signal and examines 49 features, selecting 4 for online fault detection in a pneumatic machine at 18 Hz sampling rate for pressure sensors. While the method can be applied to other machines without retraining, it has limitations, such as requiring non-overlapping actuator actions. The classification accuracy in the tested example averaged 39%. Another dissertation by Klein [29] demonstrates the potential of using novelty scores and machine learning for fault detection in a single servopneumatic welding gun with high accuracy (up to 100%). Unlike the standard pneumatic drives examined in this paper, such systems typically include multiple sensors (e.g., several pressure sensors and a position sensor), which simplifies fault detection. Nevertheless, significant challenges were observed, including difficulty detecting increased friction and pronounced domain shifts when operating parameters change. These shifts can potentially make trained classification models ineffective, requiring recalibration of the fault detection system.

The aim of this paper is therefore to explore a broader range of time- and frequency-domain features for fault diagnosis of pneumatic cylinders, compare feature-based classification with neural networks and the cycle time-based method, and evaluate their applicability across different pneumatic drives and for different positions of a single pressure sensor per drive.

2. Fault Localization

Table 1 outlines the typical fault locations in pneumatic linear drive systems considered in the paper.

Table 1. Typical faults in pneumatic drive systems.

Fault	Definition and examples
External leakage	Air leakage from the actuator into the environment (locations a)-b) in Figure 1). Possible causes: ▪ Mechanical damage to the hose or hose aging; ▪ Damaged/worn cylinder wiper; ▪ Loosened/damaged push-in fittings.
Internal leakage	Interchamber leakage (location c) in Figure 1). Possible causes: ▪ Damaged/worn cylinder piston sealing. ▪ Piston detachment from the rod
Increased friction	Additional external force (location d) in Figure 1). Possible causes: ▪ Damaged/worn cylinder piston sealing and/or wiper; ▪ Changed friction conditions of mechanical components (e.g., guide wear or contamination).

Figure 1 illustrates potential fault locations in a standard pneumatic drive with meter-out throttling. To detect the faults from Table 1 with minimal amount of sensors, different positions for the single pressure sensor position shown in Figure 1 (placements 1) and 2)) are proposed.

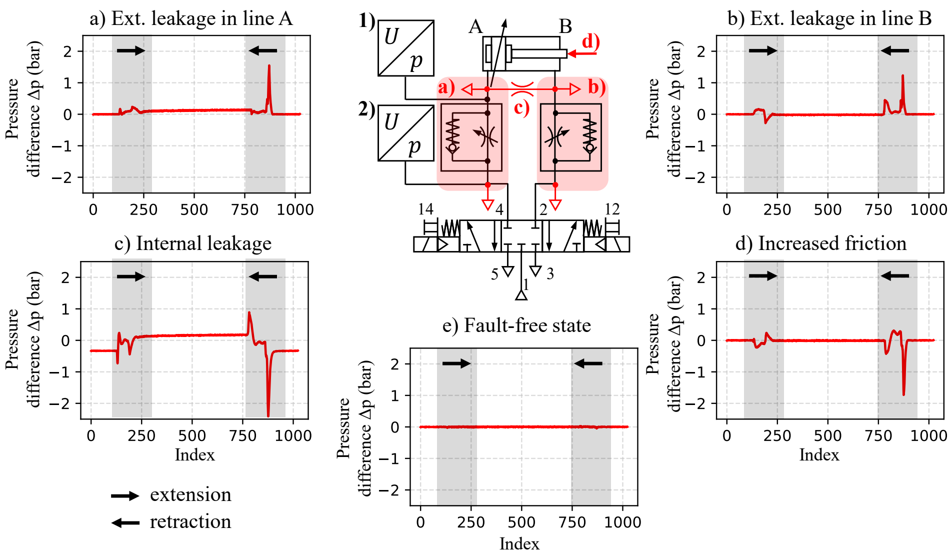

Figure 1. Considered single pressure sensor positions 1) and 2) within a pneumatic drive and potential fault locations a)-d) with corresponding exemplary patterns in pressure difference signals when measured at sensor position 1)

The basic idea behind monitoring the linear drive presented here is to observe the piston-side pressure p_A continuously or periodically. This involves comparing the reference pressure profile recorded once after commissioning and setup with the repeatedly measured current pressure profile. This results in differential pressure profiles $\Delta p = p_{A,Curr} - p_{A,Ref}$ exemplary shown in Figure 1a-e, the shape of which is to be classified for fault detection and localization.

In the case of leakage in line A, a clear permanent deviation from zero is observed during the standstill in the cylinder's extended state. Corresponding deviations also occur during extension and retraction due to the changed movement time. The deviation is more pronounced during the return stroke, where leakage A accelerates motion due to the quick exhaust effect (see [25]).

Leakage in line B and increased friction also lead to a deviation in extension and retraction times, visible as distinct peaks in the differential pressure signal. Internal leakage alters the pressure profile more severely, leading to significant distortions in the differential pressure signal. In the reference case, by contrast, deviations from zero are absent or minimal, occurring only due to sensor noise or operating fluctuations.

3. USE CASES

For the classification training, measurement data corresponding to fault-free and faulty scenarios was generated on the test bench shown in Figure 2 using the Festo DSBC-32-200-PPV-A (piston diameter 32 mm, stroke 200 mm) and the Hoerbiger R6025/50 (piston diameter 25 mm, stroke 50 mm) double-acting differential cylinders. Leaks were introduced at the locations shown in Figure 1 using additional throttles, as illustrated in Figure 2. Increased friction was simulated with a Festo DSBC-L-50-200-PPV-A pneumatic cylinder (without compressed air supply) mechanically coupled to the guide of the test cylinder.

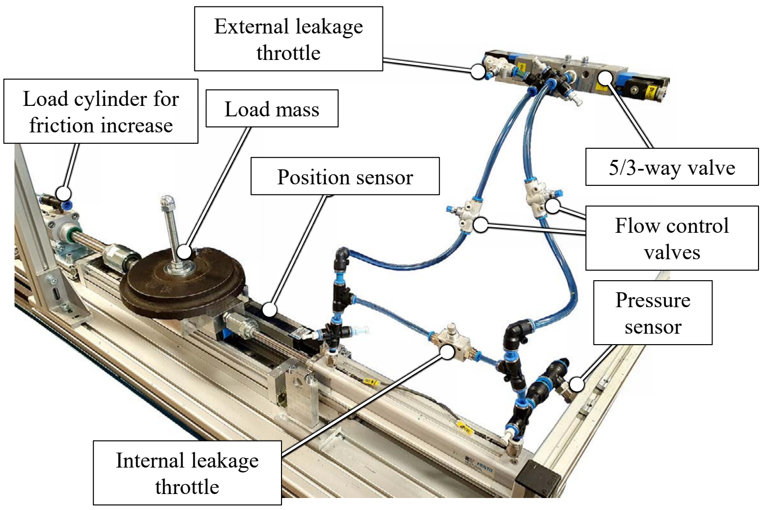

Figure 2. Test bench for pneumatic linear drives

To cover a broad range of operating conditions, the training data parameters were varied according to Table 2. The leakage throttle openings were adjusted to generate two leakage rates (20 l/min and 40 l/min under normal conditions). Throttles connected to the atmosphere at the load cylinder ports were used to generate additional counterforces, representing fault conditions equivalent to increased friction in the test cylinder. The applied throttle settings resulted in two mean counterforce levels of approximately 20 N and 40 N. These additional force levels were not determined for every operating point of the test cylinder, since the objective was to impose two distinctly different load magnitudes.

The examined drive tasks represent a classic motion task in which a load mass is moved between two positions (load cases 1-1 and 1-2 according to [7]). No pressing or mixed motion-pressing tasks were considered. Approx. 120 pressure profiles per data set were recorded, evenly split between fault-free and faulty cases shown in Figure 1, resulting in about 3000 pressure profiles for training at a 1000 Hz sampling rate. The effect of sampling rate on classification is discussed in Chapter 5.

Table 2. Training data set parameters for pneumatic linear drives

#	Piston diameter (mm)	Stroke (mm)	Hose length (m)	Operating pressure (bar abs.)	Transition time (ms)	Load mass (kg)	Pneum. frequency ratio (-)
1	25	50	5	7	450	11	1.0
2			0.5	7	250	12	1.2
3			0.5	6	500	12	2.3
4			5	6	470	10	1.0
5			0.5	6	500	6	3.2
6			0.5	7	500	12	2.5
7			5	7	800	6	2.4
8			0.5	6	250	12	1.1
9			5	7	250	0.25	3.7
10			5	6	800	6	2.2
11			5	6	250	0.25	3.4
12			0.5	7	500	6	3.5
13	32	200	0.5	6	300	12	1.2
14			5	7	800	6	3.3
15			5	7	600	6	2.5
16			0.5	7	600	12	2.6
17			0.5	7	600	6	3.6
18			5	6	690	8	2.2
19			5	6	800	6	3.0
20			5	6	700	25	1.3
21			0.5	6	600	6	3.4
22			0.5	7	300	12	1.3
23			5	7	700	27	1.4
24			0.5	6	400	6	2.2

The test data in Table 3 was collected to evaluate the classification methods on tasks involving different cylinder geometries and previously unseen operating parameters. Four leakage levels (15, 25, 30, and 40 l/min) and two friction levels (20 and 40 N) were applied. In addition to the pressure signal, cylinder motion times were recorded in the PLC to enable comparison with the cycle time-based method in the final evaluation step.

Table 3. Test data set parameters for pneumatic linear drives

#	Piston diameter (mm)	Stroke (mm)	Hose length (m)	Operating pressure (bar abs.)	Transition time (ms)	Load mass (kg)	Pneum. frequency ratio (-)
1*	50	200	1.5	7	470	31	3.8
2**	40	400	1.5	7	560	0.85	18.2
3	25	50	1.5	7	380	21	1.0

* Festo DSBC-L-50-PPV-A low-friction cylinder with adjustable pneumatic cushioning
** Festo DSBC-40-400-PPSA-N3 cylinder with self-adjusting pneumatic cushioning

4. PATTERN CLASSIFICATION

4.1. Feature-Based Classification Models

The basic procedure for training machine learning models for pattern classification is shown in Figure 3.

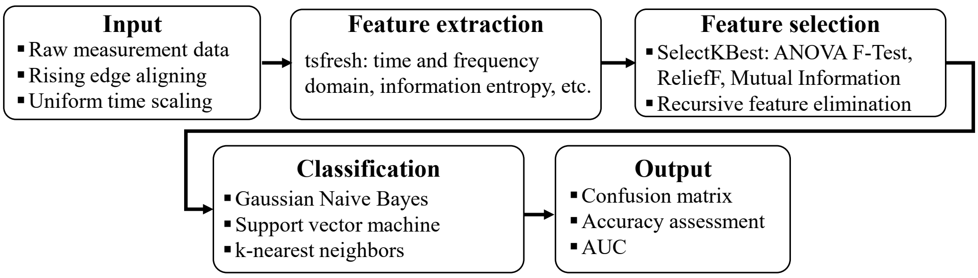

Figure 3. Pipeline for feature-based machine learning in Python

The collected raw measurement data series were singularized so that one file corresponds to a double stroke of the pneumatic cylinder, aligned and scaled to a uniform signal length of 1024 points. Next, the features of the data sets were extracted using the Python library "tsfresh", which extracts 783 features from the time and frequency domains for each profile.

In a further step, four classification models with different combinations of feature selection and classification methods shown in Table 4 were trained and evaluated. The combinations were selected based on established best practices in pattern recognition and machine learning. Filter-based feature selection methods such as ANOVA F-test, mutual information, and ReliefF are widely used with classifiers that do not perform intrinsic feature weighting, including Gaussian Naive Bayes and k-nearest neighbors [30-32]. Recursive feature elimination was combined with a linear support vector machine for classification, following the methodology proposed by Guyon et al. [33].

The training was done using a stratified group k-fold cross-validation with five folds, in which folds were defined by the experimental datasets from Table 2. This ensures that all measurements from the same datasets are assigned to either the training or the validation set, but never split across both (e.g. 1st fold contains datasets 1-5, 2nd fold contains datasets 6-10 etc.) to realistically estimate the performance of the classifier during the training. Within each fold, preprocessing included normalization of all extracted features to the interval [0;1] using min-max scaling and removal of non-informative features via variance thresholding.

Table 4. Combinations of feature selection and classification methods applied in Python for the classification models.

Model #	Feature selection method	Classification method
1	ANOVA F-test from SelectKBest	Gaussian Naive Bayes (GNB)
2	Recursive feature elimination (RFE) with feature ranking via linear support vector machine (SVM)	Linear support vector machine classifier (SVM)
3	ReliefF from SelectKBest	k-nearest neighbors (kNN) with 20 neighbors
4	Mutual information-based feature selection from SelectKBest (MI)	k-nearest neighbors (kNN) with 20 neighbors

The predictive performance of each combination was evaluated on the test data set presented in Table 3, which was not used during training and is therefore unknown to the classifier. Performance was assessed using accuracy and the area under the receiver operating characteristic curve (AUC). The average AUC across all classes indicates how effectively the classifier distinguishes between the different classes.

The described procedure was conducted once for the pressure sensor placement at the cylinder (variant 1) and once at the way valve (variant 2) as shown in Figure 1. In each case, the extension part of the pressure profile and the entire pressure profile (extension and retraction) were examined separately in order to compare performance.

4.2. Neural Network

Another method examined for classifying the pressure profile of the component involves neural networks. Similar to Chapter 4.1, the training data was aligned, scaled to a uniform signal length of 1024 points, filtered, and fed into a neural network for training in the MATLAB environment. The proposed neural network comprises 13 layers in total, including 5 learnable layers: three convolutional layers (1D-CNN) followed by a bidirectional long short-term memory layer (BiLSTM) and a fully connected layer. This allows both local patterns and their global temporal ordering to be captured in the pressure difference signal. The structure of the neural network is presented in Table 5.

The 1D convolutional layers are used as a feature extractor, enabling the detection of characteristic local patterns such as pressure slopes, inflection points, and short-term oscillations that arise from fault events. Their dilation by applying dilation factors of 1, 2, and 4 is used to progressively increase the temporal receptive field of the network while preserving the original time resolution of the signal. This three-stage design represents the minimal depth required to capture local, intermediate, and extended temporal structures without excessive model complexity. Further convolutional layers were avoided, as global temporal dependencies are subsequently modeled by a bidirectional LSTM layer.

The bidirectional LSTM layer models long-term temporal dependencies and explicitly encodes the temporal order of signal components by processing the sequence in both forward and backward directions. This is particularly important for fault patterns that are similar in amplitude but differ in the order of positive and negative pressure lobes. The final fully connected and softmax layers map the learned representation to class probabilities, while the dropout layer mitigates overfitting. Leaky ReLU activations are employed to preserve information contained in negative signal components and to ensure stable gradient propagation.

The final network depth and parametrization was determined through empirical validation. Investigations on the test dataset confirmed that a three-stage convolutional block provided the optimal balance between sufficient receptive field coverage and generalization capability.

Table 5. Neural network structure

#	Layer	Description and Parametrization
1	Sequence input layer	6 input values
2	1D convolutional layer	Local temporal patterns extraction with unchanged time length; 64 filters, kernel size 7, dilation factor 1
3	Layer normalization	Normalization of activations for training stabilization
4	Leaky ReLU	Activation function with negative slope 0.1
5	1D convolutional layer	64 filters, kernel size 7, dilation factor 2
6	Leaky ReLU	Activation function with negative slope 0.1
7	1D convolutional layer	64 filters, kernel size 7, dilation factor 4
8	Leaky ReLU	Activation function with negative slope 0.1
9	Bidirectional LSTM layer	128 neurons, forward and backward detection of time dependencies, output taken from the last time step
10	Dropout layer	Dropout rate 0.5 for regularization against overfitting
11	Fully connected layer	Maps the 256-dimensional feature vector to 5 output nodes
12	Softmax layer	Output of class probabilities
13	Classification layer	Loss function calculation and final classification

The following six values or features were used as input:

- Normalized pressure difference signal: The original signal is normalized by the global standard deviation σ of all training data
- First derivative of the normalized signal
- Positive portion of the normalized signal.
- Negative portion of the normalized signal
- Order feature: A binary feature indicating whether the first positive peak of the signal occurs before the first negative peak.
- Area ratio: The ratio of the area under the positive signal portions to the area under the negative signal portions

In addition to the normalized pressure difference signal, five auxiliary inputs are provided to embed prior pattern knowledge directly into the learning process of the neural network. The first derivative is intended to improve sensitivity to rising and falling edges. The positive and negative signal portions explicitly encode asymmetric pressure behavior, which is characteristic of different fault locations shown in Figure 1. The order feature and area ratio also directly represent physically meaningful distinctions observed in the patterns, such as a pressure increase followed by a decrease during extension vs. the inverse sequence demonstrated in Figure 1b) and d). Their direct specification through auxiliary inputs simplifies training and classification, as such relationships do not have to be implicitly recognized or derived by the neural network. Together, this multi-channel representation improves class separability, accelerates convergence, and enhances robustness against variability in real pneumatic systems.

Similar to the classification models in Chapter 4.1, the performance of the neural network was evaluated based on accuracy and AUC for two different pressure sensor positions (at the cylinder vs. at the valve) as well as for two different sections of the pressure profile (extension vs. full stroke).

5. RESULTS

5.1. Performance of Feature-Based Classification Models and the Neural Network

After applying the fault classification methods described in Chapters 4.1 and 4.2 to the test data set from Table 3, which was previously unknown to the classifiers, their performance was compared for the different sensor positions and pressure signal sections. Figure 4 and Figure 5 provide an overview of the accuracy and AUC of the feature-based classification models depending on the number of features in comparison to the neural network.

The neural network and feature-based classifiers showed comparable performance. The highest test accuracy (92.5%) was achieved by model #3 (ReliefF with k-NN) using full-stroke signals with 50 features and pressure measured at the cylinder (Figure 4c). The accuracy drop above 100 features across different classifiers indicates overfitting due to feature redundancy. Model #2 (RFE with SVM) was also highly effective, achieving neural-network-level accuracy and AUC across all settings with only five features. Using RFE, the following "tsfresh" features describing global and local changes in amplitude, periodicity, and frequency content were selected for full-stroke classification with pressure measured at the cylinder:

- `longest_strike_below_mean`: Length of the longest continuous sequence of values below the mean value.
- `sum_of_reoccurring_data_points`: Sum over all repeated observations in the time series (i.e., data points that occur more than once) in the time series.
- `fft_coefficient__attr_"angle"__coeff_77`: Phase angle of the Fourier coefficient at coefficient index 77.
- `fft_aggregated__aggtype_"skew"`: Skewness of the frequency spectrum.
- `agg_linear_trend__attr_"intercept"__chunk_len_10__f_agg_"var"`: Measures how much the baseline level of the signal (intercept of a linear trend) fluctuates between consecutive segments of length 10.

The highest accuracy was obtained when measuring the pressure directly at the cylinder. Measuring pressure at the valve reduced accuracy on average by about 11% for the extension stroke and 8% for the combined extension and retraction. This reduction is likely due to varying hose lengths, which cause more diverse pressure signals for the same fault scenarios, whereas cylinder measurements lead to more uniform patterns.

The inclusion of the return stroke (i.e., evaluation of the full stroke) increased the accuracy of the pattern classification by approx. 4.2% for the pressure measurement at the cylinder and by 6.4% for the pressure measurement at the valve the compared to the variant with extension only.

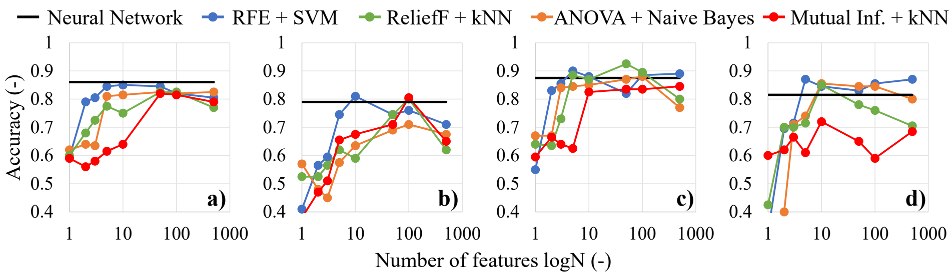

Figure 4. Classification accuracy of the neural network and feature-based models as a function of the number of features, pressure sensor location, and pressure signal segment: (a) cylinder, extension; (b) valve, extension; (c) cylinder, extension + retraction; (d) valve, extension + retraction.

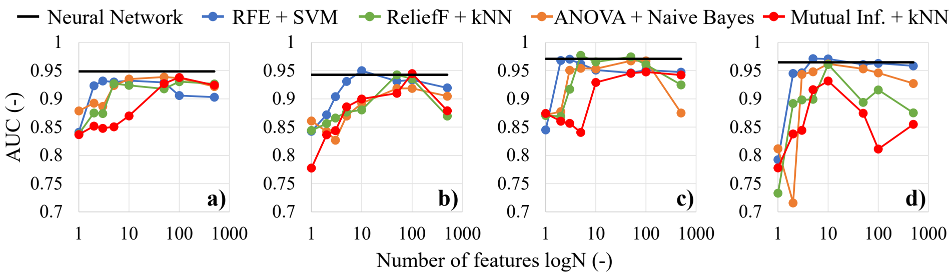

Figure 5. Area under the receiver operating characteristic curve (AUC, average value for all classes) of the neural network and feature-based models as a function of the number of features, pressure sensor location, and pressure signal segment: (a) cylinder, extension; (b) valve, extension; (c) cylinder, extension + retraction; (d) valve, extension + retraction.

Figure 6 shows the influence of the sensor's sampling rate on accuracy and AUC for two selected classification methods (RFE+SVM with 5 features vs. neural network) when measuring extension and retraction pressure profiles at the cylinder. As can be seen, it is possible to reduce the sampling rate from the original 1000 Hz to 100 Hz without significant loss of accuracy. However, further reduction of the sampling rate leads to reduced accuracy.

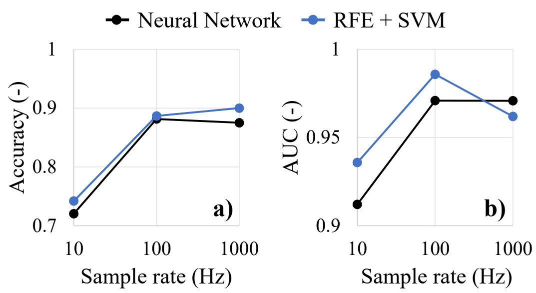

Figure 6. a) Accuracy and b) area under the receiver operating characteristic curve (AUC, average value for all classes) of neural network and classifier RFE+SVM with 5 features depending on the sampling rate of the pressure sensor; pressure measurement at the cylinder, extension and retraction

5.2. Comparison with Cycle Time-Based Method

Finally, the cycle time-based method described in [25] was also applied to the test data set from Table 3. Figure 7 presents the confusion matrices for the selected feature-based classification method and neural network when measuring extension and retraction of the cylinder and compares them with the confusion matrix of the cycle-based method.

The differentiability between the classes is comparably good both for the feature-based method and for neural network methods, with the feature-based classifier in Figure 7a being better at recognizing the error-free state of the cylinder. The cycle time-based method in Figure 7c, on the other hand, encountered difficulties when detecting and localizing minor external leaks of 15 l/min and/or external leaks occurring in the hose between the directional control valve and the throttle valve. Such leaks are particularly difficult to localize, as they often result only in a slight deviation in the cylinder's movement time. Detecting the smaller counterforce increase of 20 N was also problematic. This results in a lower accuracy of the cycle time-based method (74%) compared to the feature-based classifier (90%) and neural network (87.5%).

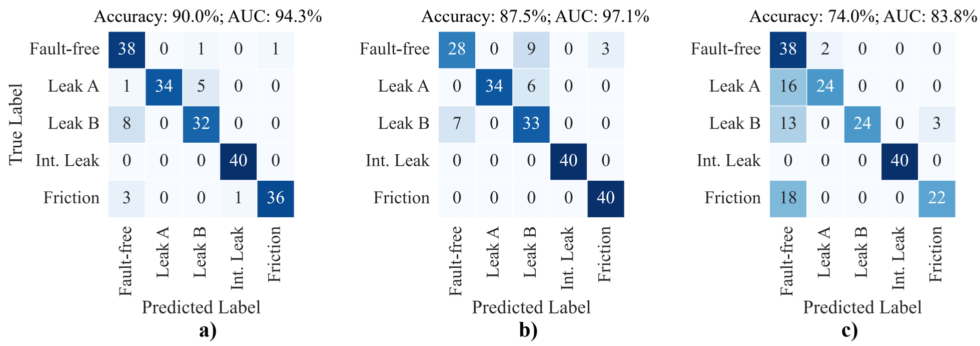

Figure 7. Confusion matrices for test data using different classification methods: a) RFE + SVM (5 features), cylinder pressure, extension + retraction; b) neural network, cylinder pressure, extension + retraction; c) cycle time-based method

6. CONCLUSIONS

This paper presents a fault detection method based on a single pressure sensor per drive combined with various classification techniques. The results show that only a few features are sufficient to detect and localize different fault scenarios with high accuracy (up to 92.5% on the test dataset). Using five features selected by recursive feature elimination and classified with the k-nearest neighbors algorithm, 90% accuracy was achieved. The developed neural network, consisting of three convolutional layers and a bidirectional long short-term memory layer, delivered comparable results. This represents a significant improvement over the cycle time-based soft-sensor method from [25], which achieved 72.4% accuracy on the same test data set. The broad applicability of the method was also confirmed: while training was conducted on cylinders with piston diameters of 25 and 32 mm, the test was performed on other cylinder sizes (40 and 50 mm) and/or under other operating conditions.

However, the method described here still has certain limitations. The current study is restricted to standard horizontal motion tasks. For broader applicability, future work should examine further load cases (e.g., considered in [7]) such as pressing tasks. The training data for various load scenarios and operating conditions can also be obtained through simulation to increase generalizability. Moreover, the method currently requires a pause between extension and retraction cycles and should be extended to continuous-motion applications. High pressure-sensor sampling rates between 100 and 1000 Hz are also necessary to achieve the reported accuracy; reducing the rate to 10 Hz decreased accuracy from 90% to 74.2%. The retrofit with pressure sensors also incurs additional costs that may exceed the cost of the proximity switches. This can be mitigated e.g. by using lower-cost sensors such as Micro-Electro-Mechanical Systems (MEMS) pressure sensors or by their mass production for integration into pneumatic actuators or valves.

Despite these constraints, the proposed method shows strong potential for deployment in typical industrial drive applications. It could be implemented in retrofittable monitoring modules at the cylinder using microcontrollers or mini-PCs, or in valve terminals already equipped with pressure sensors, such as the Festo VTEM, enabling fault detection during operation without dedicated diagnostic cycles.

7. FUNDING

This research was funded by the German Federal Ministry for Economic Affairs and Energy (BMWE), grant number 03EN4050A (OekEffDatA: Data-driven System Monitoring and Design for Ecological Efficiency in Operation).

8. REFERENCES

[1] T. Radermacher, M. Merx, A. Sitte, V. Boyko, ‘Potenzialstudie Energie-/Kosteneinsparung in der Fluidtechnik’, final report No. 37EV181030, TU Dresden, University of Stuttgart, Germany, 2021.

[2] C. R. Jimenez, O. Reinertz, K. Schmitz, ‘Dimensioning Method of Pneumatic Cylinders Based on the Pneumatic End-cushion’, Int. J. Fluid Power, 26(03), pp. 381-410, 2025. DOI:10.13052/ijfp1439-9776.2632

[3] W. Gauchel, ‘Energiesparende Pneumatik. Konstruktive sowie schaltungs- und regelungstechnische Ansätze’, O+P Fluidtechnik, pp. 33-39, 1/2006.

[4] R. Saidur, N. A. Rahim, M. Hasanuzzaman, ‘A review on compressed-air energy use and energy savings’, Renewable and Sustainable Energy Reviews, 14, pp. 1135-1153, 2010. DOI:10.1016/j.rser.2009.11.013

[5] D. D. Šešlija, I. M. Milenković, S. P. Dudić, J. I. Šulc, ‘Improving Energy Efficiency in Compressed Air Systems. Practical Examples’, THERMAL SCIENCE, Vol. 20, Suppl. 2, pp. 335-370, 2016. DOI: 10.2298/TSCI151110022S

[6] D. Gryboś, J. S. Leszczyński., ‘A Review of Energy Overconsumption Reduction Methods in the Utilization Stage in Compressed Air Systems’, Energies, 17, 1495, 2024. DOI:10.3390/en17061495

[7] V. Boyko, F. Nazarov, W. Gauchel, R. Neumann, M. Doll, J. Weber, ‘Comprehensive Application-Based Analysis of Energy-Saving Measures in Pneumatics’, Int. J. Fluid Power, 25(01), pp. 27-58, 2024. DOI:10.13052/ijfp1439-9776.2512

[8] J. Mallia, E. Francalanza, P. Xuereb, P. Refalo, 'Intelligent Approaches for Anomaly Detection in Compressed Air Systems: A Systematic Review', Machines, 11, 750, 2023. DOI:10.3390/machines11070750

[9] M. Borg, P. Refalo, E. Francalanza, 'Failure Detection Techniques on the Demand Side of Smart and Sustainable Compressed Air Systems: A Systematic Review', Energies, 16, 3188, 2023. DOI:10.3390/en16073188

[10] C. Dierolf, 'Identifikation und Klassifikation von Druckluft-Leckagen mit Methoden des maschinellen Lernens in Maschinen', PhD dissertation, Stuttgart, Germany, 2022. DOI:10.18419/opus-12124

[11] S. Fritz, 'Verfahren zur Erkennung sowie Diagnose von Fehlern in pneumatischen Systemen und Komponenten', PhD dissertation, Aachen, Germany, 2011.

[12] G. Belforte, L. Mazza, T. Raparelli, 'Analysis of Typical Failure Situations in Pneumatic Cylinders under Load', Lubrication Eng., 48(11), pp. 840–845, 1992.

[13] Festo SE & Co. KG, 'Leckageortung und -beseitigung. Energy Saving Services von Festo', Esslingen, Germany, 2018.

[14] Festo SE & Co. KG, 'Weltneuheit Festo Motion Terminal VTEM', Esslingen, Germany, 2017.

[15] Festo SE & Co. KG, 'Energieeffizienzmodul MSE6', Esslingen, Germany, 2018.

[16] AVENTICS, 'Smart Pneumatics Opportunities for Industry Through Intelligent Pneumatics', Esslingen, Germany, 2024.

[17] H. Mahmoud, F. Vlašic, P. Mazal, M. Jana, 'Leakage analysis of pneumatic cylinders using acoustic emission', Insight-Non-Destr. Test. Cond. Monit, 59, pp. 500–505, 2017. DOI:10.1784/insi.2017.59.9.500

[18] H. Mahmoud, 'Diagnosis of Pneumatic Cylinders Using Acoustic Emission Methods', PhD thesis, Brno, Czech Republic, 2017.

[19] D. Czopek, D. Gryboś, J. Leszczyński, J. Wiciak, 'Identification of energy wastes through sound analysis in compressed air systems', Energy, 239, 122122, 2021. DOI:10.1016/j.energy.2021.122122

[20] Y. Shi, J. Chang, L. Li, Y. Wang, S. Xu, Y. Niu, 'Improved object detection network for pipeline leakage localization in the pneumatic system based on thermal images', Measurement, 242, 116225, 2025. DOI:10.1016/j.measurement.2024.116225

[21] A. Muth, 'Reibkraftermittlung an pneumatischen Ventilen und Zylindern', PhD thesis, Dresden, Germany, 1997.

[22] A. Vygantas, M. Saunoris, 'Investigation of high frequency vibrations of pneumatic cylinders', Ultragarsas, 51, pp. 21–26, 2004.

[23] M. Tiboni, C. Remino, 'Condition Monitoring of Pneumatic Drive Systems Based on the AI Method Feed-Forward Backpropagation Neural Network', Sensors, 24(6), 1783, 2024. DOI:10.3390/s24061783

[24] W. Gauchel, T. Streichert, Y. Wilhelm, 'Predictive maintenance with a minimum of sensors using pneumatic clamps as an example'. Proc. of the 12th International Fluid Power Conference, Dresden, Germany, 9–11 March 2020; pp. 175–183, 2020. DOI:10.25368/2020.81

[25] V. Boyko, J. Weber, 'Cycle Time-Based Fault Detection and Localization in Pneumatic Drive Systems', Actuators, 13, 447, 2024. DOI:10.3390/act13110447

[26] J. Zubieta, U. Izagirre, L. Eciolaza, A. S. De Buruaga, L. Galdos, 'Step-time measurement: A scalable sub-cycle time defining methodology for anomaly detection and predictive maintenance in sequential production lines', J. of Manufacturing Systems, 83, pp. 1-11, 2025. DOI:10.1016/j.jmsy.2025.08.011

[27] M. Doll, R. Neumann, O. Sawodny, 'Dimensioning of pneumatic cylinders for motion tasks', Int. J. of Fluid Power, 16:1, pp. 11-24, 2015. DOI: 10.1080/14399776.2015.1012437

[28] Ž. Nakutis, P. Kaškonas, 'An approach to pneumatic cylinder on-line conditions monitoring', Mechanika, 4(72), pp. 41-27, 2008.

[29] S. Klein, 'Kombination von überwachten und teilüberwachten Methoden des maschinellen Lernens für eine adaptive und robuste Zustandsüberwachung industrieller Applikationen', PhD dissertation, Saarbrücken, Germany, 2025. DOI:10.22028/D291-44645

[30] I. Guyon, A. Elisseeff, 'An Introduction to Variable and Feature Selection', J. of Machine Learning Research, 3, pp. 1157-1182, 2003. DOI: 10.1162/153244303322753616

[31] P. Schumann, M. Scholz, K. Trentzsch, T. Jochim, G. Śliwiński, H. Malberg, T. Ziemssen, 'Detection of Fall Risk in Multiple Sclerosis by Gait Analysis—An Innovative Approach Using Feature Selection Ensemble and Machine Learning Algorithms', Brain Sci, 12, 1477, 2022. DOI: 10.3390/brainsci12111477

[32] I. Jebadurai, G. Paulraj, J. Jebadurai, S. Silas, 'Experimental analysis of filtering-based feature selection techniques for fetal health classification', Serbian J. of Electrical Engineering, 19, 2, pp. 207-224, 2022. DOI: 10.2298/SJEE2202207J

[33] I. Guyon, J. Weston, S. Barnhill, V. Vapnik, 'Gene Selection for Cancer Classification using Support Vector Machines', Machine Learning, 46, pp. 389-422, 2002. DOI:10.1023/A:1012487302797

Biographies

Vladimir Boyko holds a M.Eng. degree in Mechanical Engineering from the University of Applied Sciences Jena, Germany. Since 2018 he has been working as a research assistant at the Chair of Fluid-Mechatronic Systems (Fluidtronics), Institute of Mechatronic Engineering, TUD Dresden University of Technology, Germany. His current research fields include pneumatics, fault detection, and energy efficiency.

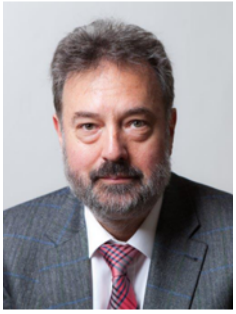

Jürgen Weber has been appointed in 2010 as a University Professor and the Chair of Fluid-Mechatronic Systems as well as the Director of the Institute of Fluid Power at the TUD Dresden University of Technology, Germany, and took on the leadership of Institute of Mechatronic Engineering in 2018. He finished his doctorate in 1991 and was an active Senior Engineer at the former Chair of Hydraulics and Pneumatics until 1997. This was followed by a 13-year industrial phase. Besides his occupation as the Head of the Department Hydraulics and Design Manager for Mobile and Tracked Excavators, starting in 2002, he took on responsibility for the hydraulics in construction machinery at CNH worldwide. From 2006 onwards, he was the Global Head of Architecture for hydraulic drive and control systems, system integration and advance development CNH construction machinery.